NOTES AND CORRESPONDENCE

Low-Frequency Variability of the Indian Monsoon–ENSO Relationship and the Tropical Atlantic: The "Weakening" of the 1980s and 1990s

F. KUCHARSKI

Earth System Physics Section, The Abdus Salam International Centre for Theoretical Physics, Trieste, Italy

A. BRACCO*

Physical Oceanography Department, Woods Hole Oceanographic Institution, Woods Hole, Massachusetts

J. H. YOO AND F. MOLTENI

Earth System Physics Section, The Abdus Salam International Centre for Theoretical Physics, Trieste, Italy

(Manuscript received 25 July 2006, in final form 13 December 2006)

ABSTRACT

The Indian monsoon–El Niño–Southern Oscillation (ENSO) relationship, according to which a drier than normal monsoon season precedes peak El Niño conditions, weakened significantly during the last two decades of the twentieth century. In this work an ensemble of integrations of an atmospheric general circulation model (AGCM) coupled to an ocean model in the Indian Basin and forced with observed sea surface temperatures (SSTs) elsewhere is used to investigate the causes of such a weakening.

The observed interdecadal variability of the ENSO–monsoon relationship during the period 1950–99 is realistically simulated by the model and a dominant portion of the variability is associated with changes in the tropical Atlantic SSTs in boreal summer.

In correspondence to ENSO, the tropical Atlantic SSTs display negative anomalies south of the equator in the last quarter of the twentieth century and weakly positive anomalies in the previous period. Those anomalies in turn produce heating anomalies, which excite a Rossby wave response in the Indian Ocean in both the model and the reanalysis data, impacting the time-mean monsoon circulation.

The proposed mechanism of remote response of the Indian rainfall to tropical Atlantic sea surface temperatures is further tested forcing the AGCM coupled to the ocean model in the Indian Basin with climatological SSTs in the Atlantic Ocean and observed anomalies elsewhere. In this second ensemble the ENSO–monsoon relationship is characterized by a stable and strong anticorrelation through the whole second half of the twentieth century.

1. Introduction

In the late 1800s Sir Gilber Walker, visiting India to investigate the causes of a series of severe droughts, discovered the Southern Oscillation (SO) and its relationship with the Indian monsoon rainfall (IMR). The fundamental physical mechanism behind the tendency for a drier than usual Indian monsoon preceding peak El Niño conditions (and vice versa for La Niña events) resides in the atmospheric teleconnection between the Pacific and Indian basin (Klein et al. 1999; Krishnamurthy and Kirtman 2003). As El Niño develops in boreal spring, subsidence over South Asia increases due to an eastward shift of the Walker circulation over the center of the Pacific; this suppresses convection over South Asia and results in a weaker summer monsoon (Walker 1924; Rasmusson and Carpenter 1983; Webster and Yang 1992; Ju and Slingo 1995, among others) while positive SST anomalies are still growing in the central and eastern Pacific. Since the late 1970s this relationship has weakened substantially (Krishna Kumar et al.

* Current affiliation: School of Earth and Atmospheric Sciences, Georgia Institute of Technology, Atlanta, Georgia.

Corresponding author address: Fred Kucharski, The Abdus Salam International Centre for Theoretical Physics, Earth System Physics Section, Strada Costiera 11, 34014 Trieste, Italy.
E-mail: kucharsk@ictp.it

DOI: 10.1175/JCLI4254.1

1999; Torrence and Webster 1999). As a notable example, the 1997/98 El Niño event, despite its intensity, produced only marginal rainfall anomalies over India.

The drop in correlation between ENSO and the IMR has been tentatively attributed to a broad range of phenomena, ranging from changes in the atmospheric fields due to global warming (Krishna Kumar et al. 1999) to natural low-frequency atmospheric variability (Krishnamurthy and Goswami 2000); from changes in the atmospheric circulation in the North Pacific (Kinter et al. 2002) or in the North Atlantic and consequently in the Eurasian snow cover (Chang et al. 2001) to variability of the Pacific decadal oscillation (Krishnan and Sugi 2003); and from changes in the atmospheric and oceanic teleconnection patterns between the Pacific and Indian basins associated with ENSO characteristics pre and post the climatic shift in 1976 (Annamalai and Liu 2005; Annamalai et al. 2005) to stochastic noise (Gershunov et al. 2001) and, finally, to the co-occurrence of ENSO and the so-called Indian Ocean Zonal Mode (IOZM) (Saji et al. 1999; Webster et al. 1999). The existence of the IOZM as an independent coupled mode of variability of the Indian Ocean, its relation with ENSO, and its impact on the IMR have been subject of an intense debate in the last five years (Iizuka et al. 2000; Allan et al. 2001; Baquero-Bernal et al. 2002; Saji and Yamagata 2003; Annamalai et al. 2003; Fisher et al. 2005) and consensus has not been reached so far.

Likely most of (if not all) the proposed mechanisms above are simultaneously at work and a "planetary-scale prospective" has to be taken when investigating both ENSO and monsoon dynamics (Chen 2003). However, it is useful trying to identify what physical process(es) contributed most to the recent changes in the ENSO–monsoon relationship, as a clear picture has not emerged so far. A successful attempt would be beneficial to seasonal forecasting studies and to the analysis of future climate scenarios projections. Unfortunately, it is very difficult to distinguish between the various theories using only observational datasets: the signatures of all the proposed hypotheses are most likely mixed together and the statistical significance of the analysis is questionable due to the limited time coverage of reliable reanalysis products. An alternative way to address the problem is to construct a series of ad hoc modeling experiments to test the various hypotheses. Atmospheric general circulation models (AGCMs), however, may not be adequate to assess the variability of the ENSO–monsoon relationship due to their inability to simulate the observed anticorrelation, as shown in two separate model intercomparison studies (Sperber and Palmer 1996; Wang et al. 2004). Coupled air–sea feedbacks are important over the Indian Ocean, where SST anomalies mostly originate from surface heat fluxes and cannot be simply assumed as drivers of the atmospheric variability (Lau and Nath 2000, 2003; Wu and Kirtman 2004, 2005; Wang et al. 2005; Bracco et al. 2007, referred to as B2007 hereafter). Multidecadal integrations with fully coupled GCMs are not adequate either, because the timing of particular events, such as the "climate shift" in the mid-1970s, cannot be simulated (e.g., Kinter et al. 2002).

In this paper we investigate the physical mechanisms responsible for the observed changes in the Indian monsoon–ENSO relationship using two different modeling strategies. In a first set of experiments an AGCM is forced by observed SST anomalies outside the Indian Ocean region and it is coupled to an ocean model in the Indian Basin, ensuring that coupled air–sea feedbacks are properly simulated. We will show that this configuration can reproduce the observed out-of-phase relation between ENSO and the monsoon rainfall variability and its decadal modulation during the second half of the twentieth century. In those integrations, the Indian Ocean SST variability forced remotely by ENSO is predominantly induced by heat fluxes and the observed ENSO–IOZM correlation is not reproduced, due to the absence of an oceanic bridge between the Indian and the Pacific, as already noticed in Bracco et al. (2005) and B2007.

A simple regression analysis performed on the model output and on reanalysis data identifies changes in the ENSO-forced SST variability in the tropical Atlantic as one of the major contributors to the decadal variability of the Indian monsoon–ENSO relationship. To test this hypothesis we perform a second set of integrations where climatological SSTs are imposed on the Atlantic Ocean region and observed SST anomalies force the AGCM elsewhere except over the Indian Ocean, where again the ocean model is coupled to the AGCM. The IMR interdecadal variability is not recovered in this configuration, further indicating that changes in the Atlantic play a fundamental role in modulating the rainfall response over India. The physical mechanism on which the teleconnection between the Atlantic and the Indian region is based upon is also highlighted.

A brief description of the model and of the ensemble performed is given in section 2. Results are presented in section 3. Discussion and conclusions follow in section 4.

2. Model and configurations

The model used in this study consists of the Abdus Salam International Centre for Theoretical Physics (ICTP) AGCM (Molteni 2003), nicknamed SPEEDY for simplified parameterizations and primitive equation

dynamics, in its eight-layer configuration and T30 horizontal resolution. This is coupled in the Indian Basin to the Miami Isopycnal Coordinate Ocean Model (MICOM) version 2.9 (Bleck et al. 1992) in a regional domain with 20 vertical levels and 1° × 1° horizontal resolution.

Examples of applications of the AGCM component can be found in, for example, Bracco et al. (2004) and Kucharski et al. (2006a,b).

In the first set of experiments (ENS1) the ocean model domain extends from 35°S to 30°N and from the coast of Africa to about 140°E. A 3° wide zone south of 32°S and east of 137°E is used to blend ocean model SSTs to observed values and subsurface quantities to Levitus monthly climatology. A portion of the western Pacific is included to insure that the dynamics in the Indian Basin is the least affected by the blending boundary conditions.[1] Outside the Indian Ocean the AGCM is forced with the Hadley Centre Coupled Sea Ice and SST dataset (HadISST; Rayner et al. 2003) from 1950 to 1999.

In the second ensemble (ENS2) the Atlantic Ocean SSTs are set to climatological values; otherwise, the experiment is identical to ENS1.

Each set of integrations consists of a 10-member ensemble. Different members are created by randomly perturbing the initial conditions and by performing a 20-yr spinup integration.

3. Results

a. The IMR–ENSO relation and its interdecadal variability

As a measure of the interannual variability of the Indian summer monsoon, we define an index that describes the IMR as the average June–September (JJAS) rain anomalies over land in the region 10° to 30°N and 70° to 95°E, covering most of the Indian peninsula. In Fig. 1a the IMR index calculated for the ENS1 ensemble mean is compared with the one obtained using precipitation data from the Climate Research Unit (CRU; Doherty et al. 1999).[2] Overall, the observed interannual variability is very well reproduced by the model. The standard deviations are 0.61 mm day^{-1} for the CRU data and 0.53 mm day^{-1} for the ensemble mean in ENS1. The correlation coefficient (CC) between the two indexes is 0.63, statistically significant at the 95% confidence level. Such a result is encouraging in light of the results presented by Krishna Kumar et al. (2005). In fact, the authors have analyzed the predictability of the Indian summer monsoon rainfall using large ensembles from 10 different AGCMs for the period 1950–99 and have shown that the "perfect model" skill is bounded to have median correlation around 0.65, with 60% of the simulated variance originating from internal atmospheric dynamics.

We further test the ability of the model to reproduce the observed relation between the IMR and ENSO by analyzing its evolution through the year. To this pur-

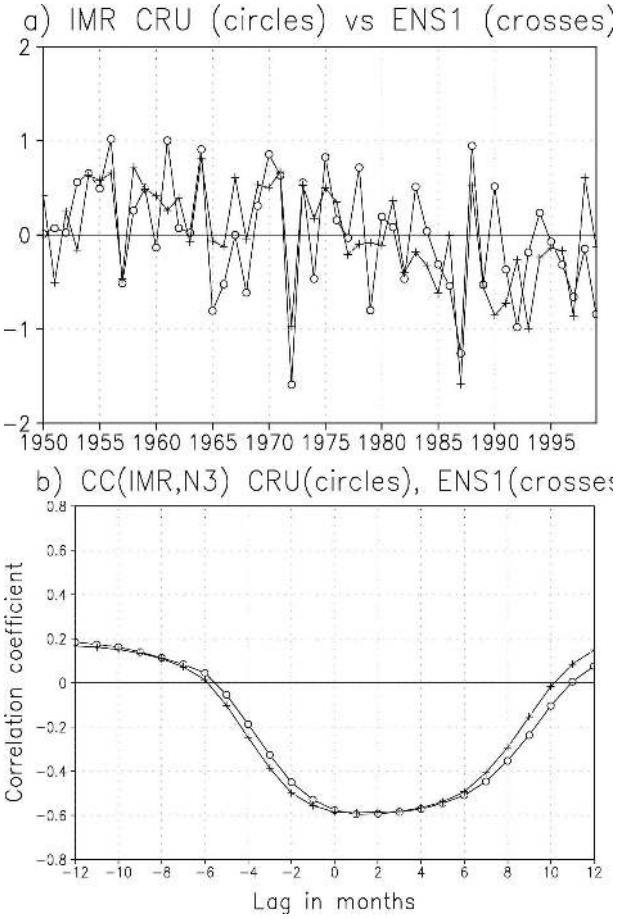

FIG. 1. (a) Time series of observed (CRU, open circles) vs ENS1 (crosses) ensemble mean Indian JJAS rain anomalies (averaged over land points of the region 10° to 30°N and 70° to 95°E). (b) Plot of the lagged correlation coefficient between the JJAS IMR and the (lagged) 4-month-averaged Niño-3 index for CRU and ENS1. Negative lags (months) mean that Niño-3 is leading IMR; positive lags mean IMR is leading the Niño-3 index. The units for (a) are mm day^{-1}.

[1] We verified the independence of our results on the inclusion of the western Pacific portion with a three-member ensemble in which the ocean model domain is limited to 110°E.

[2] We prefer to use the IMR index based on CRU data instead of the all-Indian rainfall index (Parthasarathy et al. 1995) because similar diagnostics can be applied more easily to the model results and to the gridded data. The two indexes are obviously highly correlated, with coefficient 0.85. We tested the independence of our results on the choice of the dataset.

pose we calculate the lead-lag correlations between the IMR and the Niño-3 indexes, with the last being defined as the average SST anomalies in the region 5°S to 5°N and 150° to 90°W. Figure 1b shows the lagged CC between the Indian monsoon rainfall over JJAS and the 4-month averaged Niño-3 index shifted by n months relative to the IMR for the CRU (open circles) and the ENS1 ensemble mean (crosses). Thus, in Fig. 1b the coefficient corresponding to −1 month lag refers to the correlation between JJAS IMR and the May–August Niño-3 index and so on. The seasonal modulation of the ENSO–Indian monsoon relationship is extremely well captured by the ensemble mean. Both in the model and in the observations the maximum negative correlation (around −0.6) is reached for contemporaneous indexes and for slightly positive lags (i.e., for the IMR leading the Niño-3 index by a season or so). Given the particular setup of our integrations, with observed SSTs forcing the AGCM in the Pacific, this result supports the idea that ENSO remotely influences the dynamics of the Indian summer monsoon in its development stage. This happens through changes in the heating patterns over the west and central Pacific in the spring and summer preceding the winter peak [see, e.g., Ju and Slingo (1995) for a detailed description of such a mechanism].

To further elucidate the relationship between ENSO and the IMR variabilities in observations and in the model output, Fig. 2 shows the regression pattern of the CRU (Fig. 2a) and the ENS1 ensemble mean (Fig. 2b) onto the Niño-3 index in JJAS for the 1950–99 period. All regression maps correspond to one standard deviation of the regression index. As can be clearly identified from Figs. 2a and 2b, ENSO leads to a substantial reduction of IMR in observations and in ENS1 (−0.35 mm day^{-1} for CRU and −0.42 mm day^{-1} for ENS1). The correspondence between model and observations is overall very good, with the exception of the Bay of Bengal region, where a larger than observed increase in rainfall is simulated in response to El Niño events east of the Indian peninsula, over Thailand, Laos, Cambodia, and Vietnam (and therefore outside the region of interest in this study). As found in B2007, where the model climatology and variability are analyzed in detail and in agreement with results by Wu and Kirtman (2004), a fully coupled model over the west Pacific is needed to properly simulate the latitudinal extension of convective precipitation around the south China basin.

Assuming that the model is realistically simulating the Indian monsoon precipitation and the relationship with ENSO, we perform a simple correlation analysis between the IMR and the Niño-3 indexes in JJAS over the period 1950 to 1999 and over the 25-yr intervals 1950 to 1974 and 1975 to 1999 separately. We have

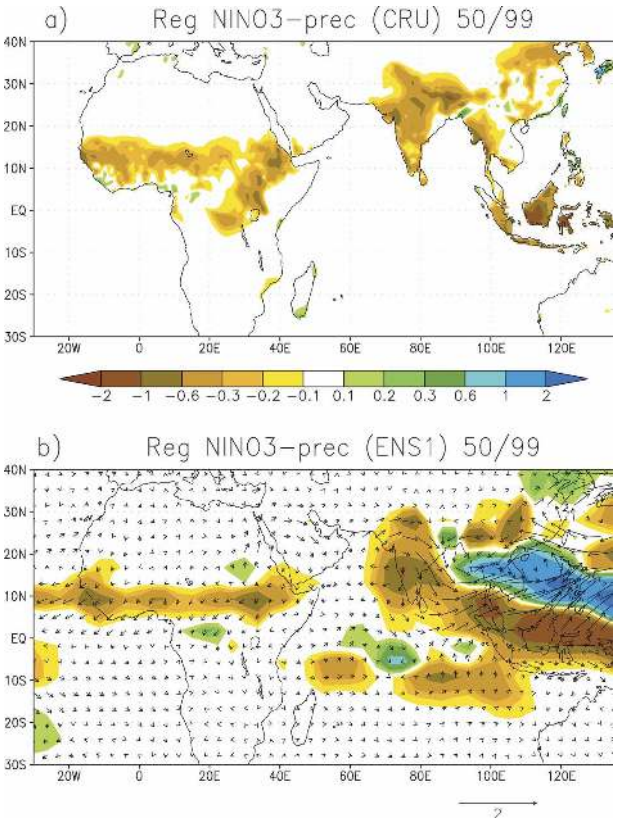

FIG. 2. Regressions onto the Niño-3 index (defined as average SST anomalies in the region 5°S to 5°N and 150° to 90°W) for the period 1950 to 1999. (a) CRU rain; (b) ENS1 ensemble mean rain and 925-hPa wind. Units are mm day^{-1} for rain in (a) and (b) and m s^{-1} for wind in (b).

chosen to consider two intervals of equal length instead of dividing our data according to the so-called climate shift of 1976/77, as such a shift cannot be considered a priori responsible for the weakening of the ENSO–monsoon teleconnection. Analogous results are obtained if 1976/77 is used instead.

Table 1 summarizes our findings. Overall the observed anticorrelation of the IMR with the Niño-3 index is well reproduced in the ensemble mean. The correlation coefficients are CC = −0.59 for CRU data and CC = −0.63 for the ENS1 ensemble average. More importantly, the weakening in the Indian monsoon–ENSO relationship observed in the last quarter of the twentieth century is well captured by the model. Indeed, when the 1975–99 period is compared to the previous 25 yr the anticorrelation reduces by an amount of 0.24 for CRU data and by an amount of 0.28 for ENS1.[3]

[3] An even stronger reduction (0.34) is found if the all-Indian rainfall dataset is used instead of CRU.

TABLE 1. Correlation coefficients (CCs) between IMR and the Niño-3 index (defined as average SST anomalies in the region 5°S to 5°N and 210° to 270°E) for CRU (top), ensemble mean of ENS1 (2d row) and mean of individual ensemble members of ENS1 (3d row), and ensemble mean of ENS2 (4th row) and mean of individual members of ENS2 (5th row) for the periods 1950–99, 1950–74, and 1975–99. The last column shows the CC difference of the later minus the earlier period for CRU and the respective experiments. Last two rows are same as above but for subperiods 1950–69 and 1980–99 for CRU and ENS1.

	1950–90	1950–74	1975–99	1975–99 − 1950–74
CC (CRU, Niño-3)	−0.59	−0.69	−0.45	0.24
CC ($ENS1_{ENSM}$, Niño-3)	−0.63	−0.79	−0.51	0.28
Mean CC (ENS1, Niño-3)	−0.42	−0.49	−0.33	0.16
CC ($ENS2_{ENSM}$, Niño-3)	−0.73	−0.74	−0.72	0.013
Mean CC (ENS2, Niño-3)	−0.49	−0.47	−0.48	−0.01
		1950–69	1980–99	1980–99 − 1950–69
CC (CRU, Niño-3)		−0.55	−0.41	0.15
CC ($ENS1_{ENSM}$, Niño-3)		−0.73	−0.56	0.17

The change in the modeled ensemble mean correlation is statistically significant at the 90% confidence level. If individual ensemble members are used, the average drop in anticorrelation is from −0.49 (1950–74 period) to −0.33 (1975–99 period), and the relative change remains about the same as for the ensemble mean. According to a *t* test the change between the two periods is statistically significant at the 95% confidence level.[4] Nine out of the 10 ensemble members show a reduction in anticorrelation between 0.1 and 0.5. One outlier displays an increase in anticorrelation of −0.24 during the last quarter of the twentieth century. As quantified by Krishna Kumar et al. (2005), internal atmospheric dynamics plays an important role in this region, and variability between the individual members has to be expected when considering changes in correlation over 25-yr periods.

To further test the independence of our results on the specific periods considered, we assess the changes in correlation between the IMR and the Niño-3 indexes for the 20-yr intervals 1980–99 and 1950–69. The results are summarized at the bottom of Table 1. Overall, the results are analogous to what was previously described, although in both CRU and ENS1 the CC changes are somewhat weaker.

The observed and simulated changes in the precipitation patterns associated with ENSO are shown in Fig. 3. Regression maps versus the Niño-3 index are calculated for each of the 25-yr intervals and the difference is plotted for the CRU data (Fig. 3a) and the ensemble mean of ENS1 (Fig. 3b), with the modeled 925-hPa wind anomalies superimposed. Over India the observed and modeled patterns are very similar, although some details in the small-scale structures are absent in the model runs, where topographic features are not well resolved due to the coarse model horizontal resolution. Over India the precipitation associated with positive ENSO events increases significantly in the latter period, both in the observations and ENS1. The average increase of the IMR in the Niño-3 regressions is 0.09 mm day^{-1} in the CRU data and 0.13 mm day^{-1} in ENS1 per standard deviation of the Niño-3 index. The difference in the surface wind regression between the two periods indicates that an anomalous cyclonic flow over India has strengthened the monsoon circulation in concomitance with positive ENSO events.

Before examining in more details the physical mechanism that is responsible for the weakening of the ENSO–IMR anticorrelation, it is worth commenting on other regions where the modeled patterns are different from the observed ones. Over the east countries of South Asia and China the model is not reproducing the observed rainfall signal. As already mentioned, a coupled model extending farther into the Pacific is indispensable to proper simulate precipitation patterns over the South China Sea. Furthermore, as discussed in Bracco et al. (2005) and B2007, the absence of an oceanic teleconnection between the Indian and the Pacific basin precludes the development of the IOZM–ENSO relation as observed. The model integrations all display a mode of variability internal to the Indian Ocean with a dynamics comparable to the one of the observed IOZM (see, e.g., Murtugudde et al. 2000; Rao et al. 2002; Gualdi et al. 2003) but independent of ENSO. The correlation between the ensemble mean IOZM, defined as in Saji et al. (1999), and the Niño-3 indexes is indeed 0.01 in JJAS and is not significant in all of the 10 members. It has been shown in Bracco et al. (2005) that whenever the OGCM domain includes the tropical Pacific the observed relation is properly simulated and

[4] To assess the statistical significance of the different means of the two ensembles of CC, we apply Fischer's *Z* transformation to the ensemble of CC for each period, then we perform a *t* test to assess that the distributions have different means.

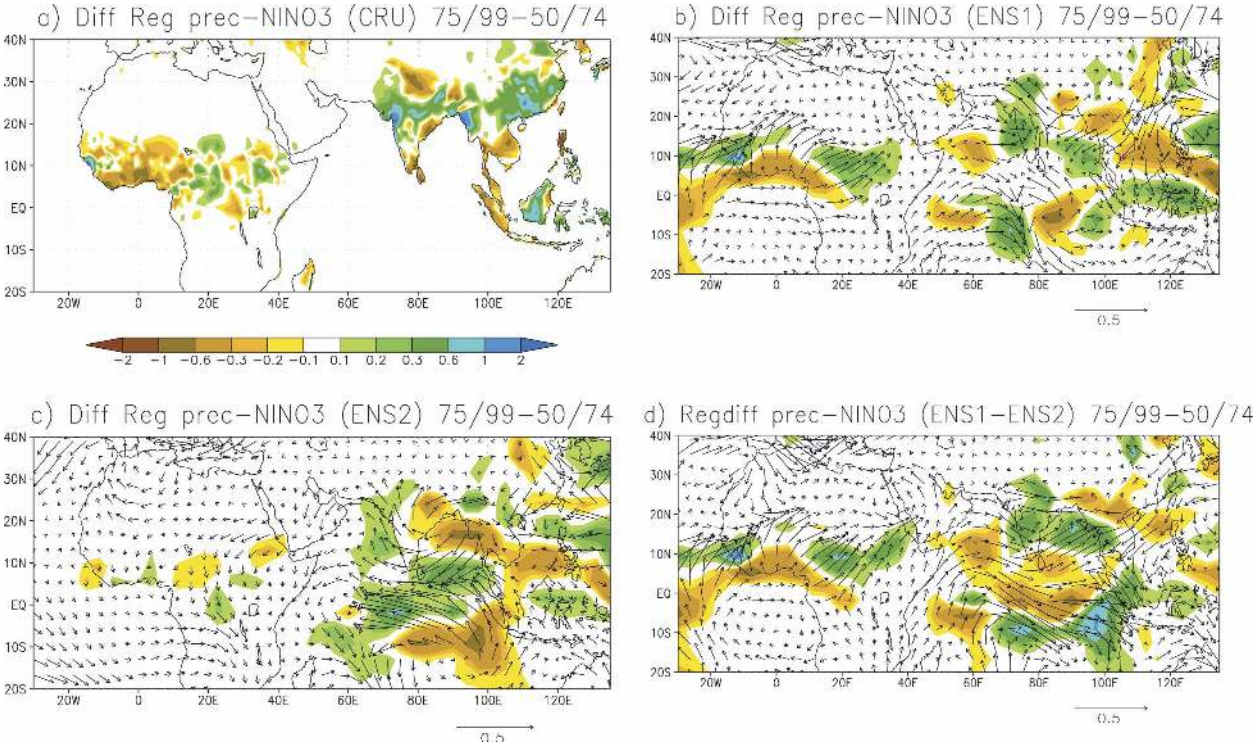

FIG. 3. The 1975–99 − 1950–74 differences of regressions of rain and 925-hPa wind onto the Niño-3 index: (a) CRU rain, (b) ENS1 ensemble mean rain and 925-hPa wind, (c) ENS2 ensemble mean rain and 925-hPa wind, (d) ENS1 − ENS2 ensemble mean rain and 925-hPa wind. Units are mm day^{-1} for rain in (a), (b), (d) and m s^{-1} for wind in (b), (c), (d).

the "oceanic bridge" between the two basins is an essential component of the IOZM–ENSO connection, as also found in Annamalai et al. (2005). The simulation of the observed IOZM–ENSO relationship is fundamental to the correct representation of the rainfall variability associated with ENSO over Indonesia and China (B2007), but from the analysis presented here it is not necessary to reproduce a large extent of the variability over India.

The independency of the internal and forced SST variability in the Indian Basin in ENS1 integrations allows for the conclusion that the modeled Indian monsoon rainfall and wind anomalies are remotely forced and associated with SST anomalies outside the Indian Ocean.

As a first step to identify the SST anomalies responsible for forcing the AGCM response, we calculate the regression coefficients of the observed SSTs versus the Niño-3 index using the HadISST dataset, including the Indian Ocean Basin. Figures 4a and 4b show the SST regression patterns in the periods 1950–74 and 1975–99 in JJAS, respectively. Figure 4c shows the difference of the SST regressions between the periods 1975–99 and 1950–74.

For the regression difference (Fig. 4c) a global patterns appears, but the dominant signal in the tropical band is found in the Atlantic region, where the cold anomalies reach values of 0.4 K between 20°S and 0°. The reason for this difference is mainly the cooling in the tropical Atlantic region in the later 1975–99 period as can be seen in Fig. 4b, with a small contribution from a warming of the tropical Atlantic in the first period 1950–74 (Fig. 4a).

No significant changes are found in the immediate proximity of the Indian peninsula, further supporting the hypothesis that the internal dynamics of the basin is not primarily responsible for the observed weakening of the ENSO–IMR relation.

b. *The role of tropical Atlantic SSTs*

The ENSO teleconnection to the tropical Atlantic has been the subject of several studies and represents a substantial part of the variability in this region (Zebiak 1993; Curtis and Hastenrath 1995; Latif and Barnett 1995; Enfield and Mayer 1997; Giannini et al. 2001, Huang et al. 2002; Huang et al. 2004, among others). Chiang et al. (2000) and more recently Münnich and Neelin (2005) analyzed interdecadal changes in the pat-

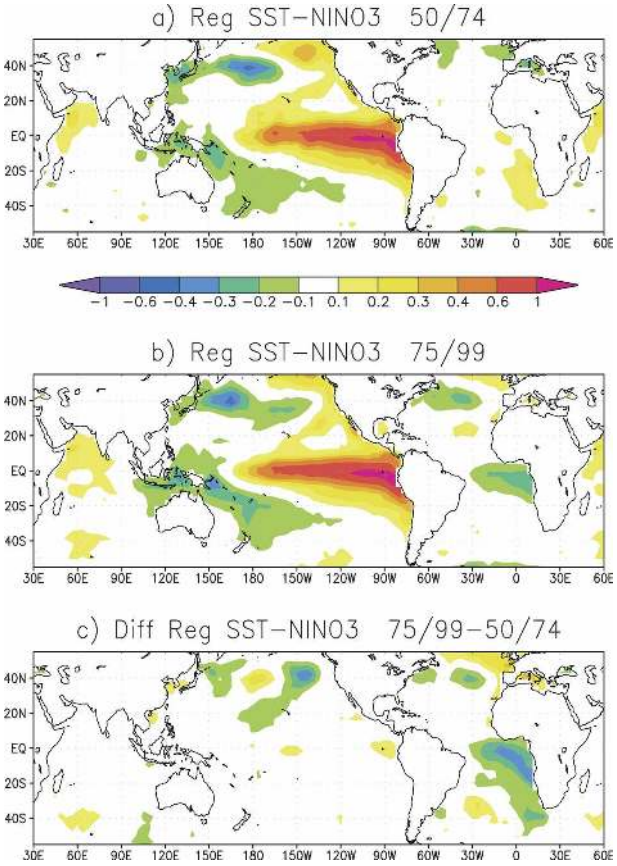

FIG. 4. Regressions and regression differences of SSTs onto the Niño-3 index: (a) 1950–74, (b) 1975–99, (c) 1975–99 − 1950–74 difference of regressions. Units are K.

terns of such teleconnection in late spring and summer and the implications for the South America rainfall variability. Both works noticed that during the 1980s and 1990s the link between the Pacific and Atlantic ITCZs has been strong, while it was nonexistent in the 1950s and 1960s, possibly resulting from the significant increase in the ENSO variance during the last quarter of the twentieth century. Chang et al. (2006), however, supported by the numerical results of Huang (2004), emphasized that fluctuations in the equatorial Atlantic depend not only on the conditions of the tropical Pacific but also on the state of the upper ocean in the Atlantic itself.

The cooling of the tropical Atlantic is responsible for a northward shift of the ITCZ over Africa (Latif and Barnett 1995; Giannini et al. 2001). Results in Fig. 3b suggest that it may also influence the monsoon circulation over India. To further investigate the role of the Atlantic SSTs, in the ENS2 ensemble SST anomalies in the Atlantic Ocean region are set to zero and climatological values are used to force the AGCM in a longitude band from about 70°W to 30°E. Otherwise, ENS2 is identical to ENS1. The resulting CC between the observed and ensemble mean IMR drops from 0.63 to 0.54 for the 1950 to 1999 period. Considering individual ensemble members the reduction in the average CC is from 0.43 in ENS1 to 0.35 in ENS2 and this change is statistically significant at the 95% level. This suggests that important information for the IMR variability resides in the Atlantic SST anomalies.

Furthermore, the correlation coefficient between the ENS2 ensemble mean IMR and the Niño-3 index is strong (−0.73) and does not vary significantly during the interval considered (0.013 as compared to 0.28 in the case of ENS1; see Table 1). For the mean of individual ensemble members, the change of CC during the last two quarters of the twentieth century is even slightly negative (CC changes in individual ENS2 members range from −0.32 to 0.26) and so is the ensemble mean precipitation change over the IMR region (−0.04 mm day^{-1}). On the other hand, the differences between ENS2 and ENS1 are statistically significant at the 90% confidence level.

Figure 3c shows the differences in the regressions for rain and 925-hPa wind of ENS2 in analogy to those shown in Fig. 3b for ENS1. Clearly, the patterns in the two ensembles differ significantly. In the absence of the Atlantic Ocean SST anomalies the regression pattern changes sign over India, providing still slightly positive values over west India but stronger negative values over east India and Bangladesh. This extends over the Indian Ocean with a strong dipolar structure in the precipitation field and a corresponding wind response. A somewhat similar feature occupies the eastern Indian Ocean in ENS1 as well (Fig. 3b) but is much weaker. From this simple analysis it appears that the Atlantic SST anomalies act to counteract the ENSO-forced response in the Indian Ocean during the last 25 yr of the twentieth century.

To isolate the effect of the Atlantic SST anomalies in Fig. 3d we show the difference in the patterns of Figs. 3b and 3c (ENS1 − ENS2). Not surprisingly, over Africa the pattern of Fig. 3d is very similar to that of Fig. 3b. However, the impact of the Atlantic is not limited to Africa and penetrates into the Indian Ocean, where it induces a strong westerly flow, and over the Indian peninsula, where a cyclonic flow enhances the monsoonal circulation, reducing the anticorrelation between ENSO and IMR indexes. Indeed, the average precipitation change between the two ensembles in the IMR region is 0.17.

To further assess the hypothesis that Atlantic SSTs influence the Indian monsoon variability, we calculate the regression coefficients of rainfall onto an index de-

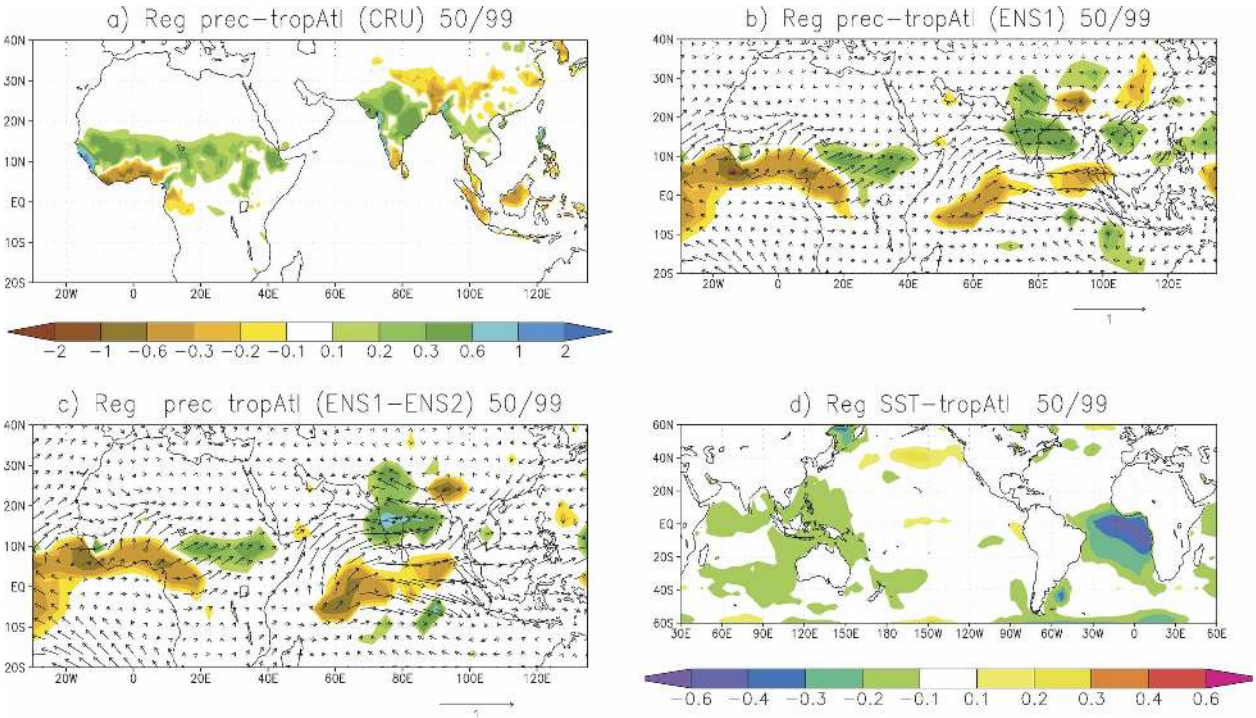

FIG. 5. Regressions of rain and SSTs onto a tropical Atlantic index defined as negative average SST anomalies in the region 20°S to 0° and 30°W to 20°E. (a) CRU rain, (b) ENS1 ensemble mean rain and 925-hPa wind, (c) ENS1 − ENS2 ensemble mean rain and 925-hPa wind, and (d) SSTs. Units are mm day^{-1} for rain in (a)–(c) and m s^{-1} for wind in (b) and (c); units for (d) are K.

fined as the *negative* of the area-averaged SST anomalies in the south tropical Atlantic in the region between 20°S to 0° and 30°W to 20°E (referred to as the tropical Atlantic index hereafter). In the CRU data (Fig. 5a) and ENS1 (Fig. 5b), the aforementioned northward shift of the ITCZ can be identified (for ENS1 only contours that are statistically significant at a 95% confidence level according to a two-tailed *t* test are plotted). In ENS1 the shift of the ITCZ extends into the Indian Ocean and farther into the Indian peninsula and causes a cyclonic surface wind anomaly similar to that of Fig. 3b. The average IMR anomaly associated with the tropical Atlantic index is 0.15 mm day^{-1} for CRU data and 0.18 mm day^{-1} for the ENS1 ensemble mean.

Additionally, the regression of SSTs onto this index (Fig. 5d) displays a pattern similar to the one in Fig. 4c. Overall, the regression pattern of Fig. 5b is very similar to Fig. 3d, where the Atlantic effect is isolated by considering the difference of ENS1 and ENS2.

Finally, the role of the Atlantic SST variability can be isolated by calculating the regression of the ensemble mean difference (ENS1 − ENS2) of rain and 925-hPa wind onto the tropical Atlantic index (Fig. 5c; again only differences that are statistically significant at the 95% confidence level are displayed). The resulting pattern is very similar to that of ENS1, confirming that it is induced by the Atlantic SST variability.[5]

The correlation of the tropical Atlantic index with the Niño-3 index is small and not significant if the interval 1950–99 is considered (CC = 0.08). However, it varies from CC = −0.22 in the period 1950 to 1974 to CC = 0.41 in the period 1975 to 1999. Such a drastic change of 0.63 is statistically significant at the 95% confidence level.

Figures 5a–c could suggest that tropical Atlantic SST anomalies influence substantially the IMR on an interannual basis. However, the amplitudes of the regressions seen in Fig. 5 are small with respect to the absolute Niño-3 regressions (Fig. 2). Indeed, the correlation coefficient of the tropical Atlantic index with IMR are only 0.24 and 0.25 for CRU data and the ENS1 ensemble mean, respectively. Therefore, the overall influence of tropical Atlantic SST anomalies on the Indian monsoon is weaker than that of ENSO, but the interdecadal variability of the SSTs over the tropical Atlan-

[5] This may seem to be a trivial result, but it is not because SST anomalies outside the Atlantic region that covary with the tropical Atlantic index may influence the IMR. Figure 5c shows that this is not the case.

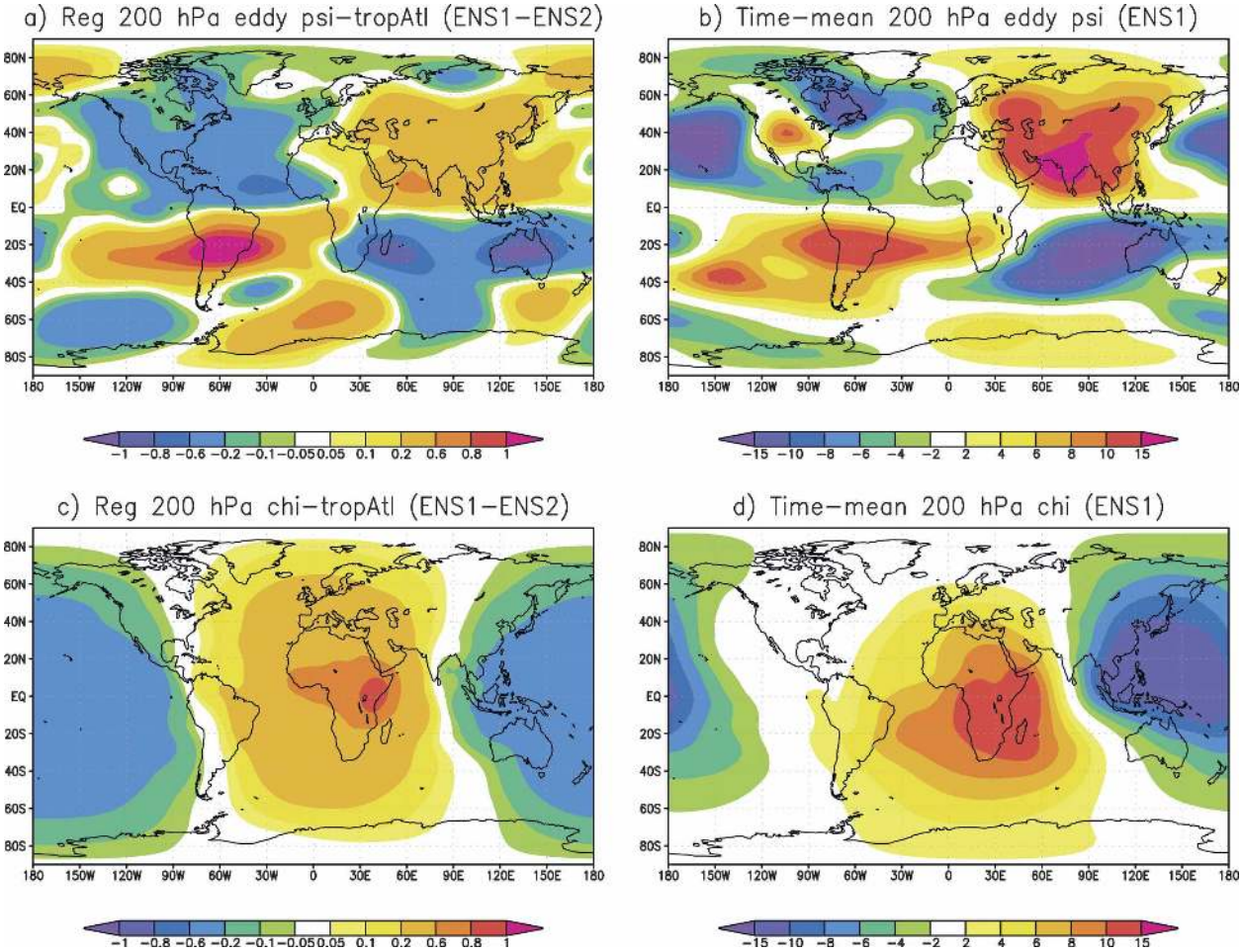

FIG. 6. (a) Regression of the 200-hPa eddy streamfunction of the ENS1 − ENS2 ensemble mean onto a tropical Atlantic index defined as negative average SST anomalies in the region 20°S to 0° and 30°W to 20°E. (b) Time-mean 200-hPa eddy streamfunction of ENS2. (c) Regression of the 200-hPa velocity potential of the ENS1 − ENS2 ensemble mean onto a tropical Atlantic index; (d) time-mean 200-hPa velocity potential. Units are 10^6 m^2 s^{-1}.

tic plays a key role in modulating the strength of the ENSO–IMR relation.

c. *Physical mechanism for tropical Atlantic–IMR teleconnection*

The physical mechanism by which the tropical Atlantic influences the Indian monsoon rainfall can be highlighted by considering the distribution of the regression coefficients of the ensemble average 200-hPa eddy streamfunction (ψ) of ENS1 − ENS2 (therefore isolating the effect of the Atlantic Ocean SSTs) onto the tropical Atlantic index in JJAS (Fig. 6a). In the equatorial region the propagation of Rossby waves to the north is substantially suppressed and the Rossby wave response pattern is trapped in the Tropics. The structure of the response in Fig. 6a is in the form of a quadruple pattern centered over equatorial Africa and is very similar to the one found by Ting and Yu (1998) in a simple baroclinic model for the June–August season (see, e.g., their Fig. 13. In their study the most efficient region for exciting this kind of response was found to be the central Pacific.) Over the northern part of the Indian Ocean and the Arabic Sea an anticyclone dominates the regression pattern at 200 hPa. This feature has a baroclinic vertical structure with a cyclone at lower levels slightly west of India, evident in the 925-hPa wind regression of Fig. 5c. Such a cyclone enhances the monsoon circulation over the Indian peninsula. This is consistent with the fact that the ψ regression in Fig. 6a projects positively onto the ENS1 mean streamfunction field shown in Fig. 6b for the period 1950 to 1999, which is similar to the observed time-mean eddy ψ (e.g., Chen 2003).

Figures 6c and 6d augment this interpretation by

showing that the 200-hPa velocity potential response (Fig. 6c, where a maximum suggests upper-level convergence and a minimum indicates divergence) also projects onto the time-mean velocity potential of ENS1 (Fig. 6d). The cooling of the tropical Atlantic Ocean causes upper-level convergence that is compensated by upper-level divergence in the surroundings. Note that the Indian monsoon region lies in the strongest gradient of the time-mean velocity potential (Fig. 6d), as suggested by Chen (2003).

4. Discussion and conclusions

In this work we analyzed the interannual variability of the Indian monsoon rainfall, focusing on its relation to the El Niño–Southern Oscillation both in the observations and in an atmospheric general circulation model regionally coupled to an ocean model over the Indian Ocean Basin.

We have shown that the observed interannual IMR variability can be realistically reproduced in our AGCM, within the limitations of the model horizontal resolution. The model is able to simulate both the observed Indian monsoon–ENSO relation and the variability observed over the second half of the twentieth century. The ad hoc modeling strategy allows us to investigate the forced component of the IMR variability. The only AGCM forcing included in the integrations are the SST anomalies outside the Indian Ocean region. Within the Indian Basin the coupled ocean model reproduces an internal mode of variability with the characteristics of the Indian Ocean Zonal Mode but independent of ENSO. In such a model, the SST variability forced by ENSO within the Indian Basin is small and does not display significant interdecadal changes over the second half of the twentieth century (B2007). SST anomalies outside the Indian Ocean domain must therefore be responsible for the interdecadal variability of the ENSO–Indian monsoon relationship in our simulations.

In those experiments, the most important contributor to the interdecadal variability of the ENSO–Indian monsoon relationship appears to be the tropical Atlantic Ocean. The analysis of the HadISST dataset reveals that the ENSO–SST teleconnection pattern has changed over the last quarter of the twentieth century compared to the previous 25 yr, with maximum differences occurring in the tropical Atlantic region, as also noted in the recent work by Münnich and Neelin (2005). Those changes are responsible for weakening the ENSO–monsoon relationship in our simulations.

Negative SST anomalies in the south equatorial tropical Atlantic are indeed co-occurring with ENSO in boreal summer in the last quarter of the twentieth century relative to the previous 25 yr, inducing heating anomalies and a Rossby wave response in the Tropics. Over the Indian Ocean the Rossby wave projects onto the time-mean pattern of the circulation, thus enhancing the time-mean Indian summer monsoon. This interpretation is supported by a second ensemble, equivalent to the first one, but with climatological SST in the Atlantic Ocean. In this second ensemble the ENSO–IMR anticorrelation is stable and strong over the whole period considered and does not display any significant interdecadal variability.

Two caveats should be attached to the analysis presented. First, the spread in the change of correlation between the Niño-3 and the IMR indexes among individual ensemble members is quite large (ranging from 0.1 to 0.5 for 9 members, with one outlier of −0.24) due to the important role that internal atmospheric variability plays in this region. Second, the pattern of rainfall changes in the ensemble average (and for the individual members) agrees with the CRU data over the central and western Indian peninsula but does not reflect the observed changes over Bangladesh and the countries surrounding the South China Sea. In the regionally coupled simulations (ENS1) the observed relation between ENSO and the Indian Ocean Zonal Mode is not simulated, because of the absence of subsurface connections between the Indian and Pacific Oceans (Bracco et al. 2005). The IOZM influences the monsoon rainfall over South and East Asia and enhances the meridional Indian monsoon circulation (Slingo and Annamalai 2000; Annamalai and Liu 2005, among others). In ENS1 we cannot expect to reproduce all of the features of the observed patterns because we are missing one of the dynamical factors that can modify the impacts of ENSO on the monsoon precipitation.

In summary, we have shown that the interdecadal variability of the ENSO–Indian monsoon relationship is, to a significant extent, modulated via the tropical Atlantic route. In this work we cannot assess the causes for the observed changes in the ENSO–SST teleconnection in the Atlantic region. They may result from natural, internal variability of the chaotic climate system, or may be due to changes in the ENSO properties following the climate shift that occurred in the mid-1970s. The analysis of the interdecadal variability in the tropical Atlantic in a coupled model will be the subject of a future study.

Acknowledgments. The experiments in this paper were performed as a contribution to the ENSEMBLES project funded by the European Commission's 6th Framework Programme, Contract GOCE-CT-2003-

505539, and as a contribution to the "International Climate of the 20th Century Project" (C20C), coordinated by the Hadley Centre for Climate Prediction and Research (United Kingdom) and the Center for Ocean–Land–Atmosphere Studies (Calverton, Maryland). A.B. is supported by the Ocean and Climate Change Institute at the Woods Hole Oceanographic Institution.

The authors wish to thank Alessandra Giannini and Marcello Barreiro for useful discussions during preparation of the manuscript. Ben Kirtman and two anonymous referees helped to improve the manuscript with valuable comments and suggestions.

REFERENCES

Allan, R. J., and Coauthors, 2001: Is there an Indian Ocean dipole, and is it independent of the El Niño–Southern Oscillations? *CLIVAR Exchanges,* Vol. 6, No. 3, 18–22.

Annamalai, H., and P. Liu, 2005: Response of the Asian summer monsoon to changes in El Niño properties. *Quart. J. Roy. Meteor. Soc.,* **131,** 805–831.

——, R. Murtugudde, J. Potemra, S. P. Xie, P. Liu, and B. Wang, 2003: Coupled dynamics over the Indian Ocean: Spring initiation of the zonal mode. *Deep-Sea Res. II,* **50,** 2305–2330.

——, J. Potemra, R. Murtugudde, and J. P. McCreary, 2005: Effect of preconditioning on the extreme climate events in the tropical Indian Ocean. *J. Climate,* **18,** 3450–3469.

Baquero-Bernal, A., M. Latif, and S. Legutke, 2002: On dipole-like variability of sea surface temperature in the tropical Indian Ocean. *J. Climate,* **15,** 1358–1368.

Bleck, R., C. Rooth, D. Hu, and L. Smith, 1992: Salinity-driven thermocline transients in a wind- and thermocline-forced isopycnic coordinate model of the North Atlantic. *J. Phys. Oceanogr.,* **22,** 1486–1505.

Bracco, A., F. Kucharski, K. Rameshan, and F. Molteni, 2004: Internal variability, external forcing and climate trends in multi-decadal AGCM ensembles. *Climate Dyn.,* **23,** 659–678.

——, ——, F. Molteni, W. Hazeleger, and C. Severijns, 2005: Internal and forced modes of variability in the Indian Ocean. *Geophys. Res. Lett.,* **32,** L12707, doi:10.1029/2005GL023154.

——, ——, ——, ——, and ——, 2007: A recipe for simulating the interannual variability of the Asian summer monsoon and its relation with ENSO. *Climate Dyn.,* **28,** 441–460.

Chang, C.-P., P. Harr, and J. Ju, 2001: Possible roles of Atlantic circulations on the weakening Indian monsoon rainfall–ENSO relationship. *J. Climate,* **14,** 2376–2380.

Chang, P., Y. Fang, R. Saravanan, L. Ji, and H. Seidel, 2006: The cause of the fragile relationship between the Pacific El Niño and the Atlantic Niño. *Nature,* **443,** 324–328.

Chen, T.-C., 2003: Maintenance of summer monsoon circulation: A planetary-scale perspective. *J. Climate,* **16,** 2022–2037.

Chiang, J. C. H., Y. Kushnir, and S. E. Zebiak, 2000: Interdecadal changes in the eastern Pacific ITCZ variability and its influence on the Atlantic ITCZ. *Geophys. Res. Lett.,* **27,** 3687–3690.

Curtis, S., and S. Hastenrath, 1995: Forcing of anomalous sea surface temperature evolution in the tropical Atlantic during Pacific warm events. *J. Geophys. Res.,* **100,** 15 835–15 847.

Doherty, R. M., M. Hulme, and C. G. Jones, 1999: A gridded reconstruction of land and ocean precipitation for the extended tropics from 1974–1994. *Int. J. Climatol.,* **19,** 119–142.

Enfield, D. B., and D. A. Mayer, 1997: Tropical Atlantic sea surface temperature variability and its relation to El Niño–Southern Oscillation. *J. Geophys. Res.,* **102,** 929–946.

Fisher, A. S., P. Terray, E. Guilyardi, S. Gualdi, and P. Delecluse, 2005: Two independent triggers for the Indian Ocean dipole/zonal mode in a coupled GCM. *J. Climate,* **18,** 3428–3449.

Gershunov, A., N. Schneider, and T. Barnett, 2001: Low-frequency modulation of the ENSO–Indian monsoon rainfall relationship: Signal or noise? *J. Climate,* **14,** 2486–2492.

Giannini, A., J. C. H. Chiang, M. A. Cane, Y. Kushnir, and R. Seager, 2001: The ENSO teleconnection to the tropical Atlantic Ocean: Contribution to remote and local SSTs to rainfall variability in the tropical Americas. *J. Climate,* **14,** 4530–4544.

Gualdi, S., E. Guilyardi, A. Navarra, S. Masina, and P. Delecluse, 2003: The interannual variability in the tropical Indian Ocean as simulated by a CGCM. *Climate Dyn.,* **20,** 567–582.

Huang, B., 2004: Remotely forced variability in the tropical Atlantic Ocean. *Climate Dyn.,* **23,** 133–152.

——, P. S. Schopf, and Z. Pan, 2002: The ENSO effect on the tropical Atlantic variability: A regionally coupled model study. *Geophys. Res. Lett.,* **29,** 2039, doi:10.1029/2002GL014872.

——, ——, and J. Shukla, 2004: Intrinsic ocean–atmosphere variability of the tropical Atlantic Ocean. *J. Climate,* **17,** 2058–2077.

Iizuka, S., T. Matsuura, and T. Yamagata, 2000: The Indian Ocean SST dipole simulated in a coupled general circulation model. *Geophys. Res. Lett.,* **27,** 3369–3372.

Ju, J., and J. M. Slingo, 1995: The Asian summer monsoon and ENSO. *Quart. J. Roy. Meteor. Soc.,* **121,** 1133–1168.

Kinter, J. L., III, K. Miyakoda, and S. Yang, 2002: Recent change in the connection from the Asian monsoon to ENSO. *J. Climate,* **15,** 1203–1215.

Klein, S. A., B. J. Soden, and N.-C. Lau, 1999: Remote sea surface temperature variations during ENSO: Evidence for a tropical atmospheric bridge. *J. Climate,* **12,** 917–932.

Krishna Kumar, K., B. Rajagopalan, and M. A. Cane, 1999: On the weakening relationship between the Indian monsoon and ENSO. *Science,* **284,** 2156–2159.

——, M. Hoerling, and B. Rajagopalan, 2005: Advancing dynamical prediction of Indian monsoon rainfall. *Geophys. Res. Lett.,* **32,** L08704, doi:10.1029/2004GL021979.

Krishnamurthy, V., and B. N. Goswami, 2000: Indian monsoon–ENSO relationship on interdecadal timescale. *J. Climate,* **13,** 579–595.

——, and B. P. Kirtman, 2003: Variability of the Indian Ocean: Relation to monsoon and ENSO. *Quart. J. Roy. Meteor. Soc.,* **129,** 1623–1646.

Krishnan, R., and M. Sugi, 2003: Pacific decadal oscillation and variability of the Indian summer monsoon rainfall. *Climate Dyn.,* **21,** 233–242.

Kucharski, F., F. Molteni, and A. Bracco, 2006a: Decadal interactions between the western tropical Pacific and the North Atlantic Oscillation. *Climate Dyn.,* **26,** 79–91.

——, ——, and J. H. Yoo, 2006b: SST forcing of decadal Indian monsoon rainfall variability. *Geophys. Res. Lett.,* **33,** L03709, doi:10.10029/2005GL025371.

Latif, M., and T. P. Barnett, 1995: Interaction of the tropical oceans. *J. Climate,* **8,** 952–964.

Lau, N. C., and M. J. Nath, 2000: Impact of ENSO on the variability of the Asian–Australian monsoons as simulated in GCM experiments. *J. Climate,* **13,** 4287–4309.

——, and ——, 2003: Atmosphere–ocean variations in the Indo-Pacific sector during ENSO episodes. *J. Climate,* **16,** 3–20.

Molteni, F., 2003: Atmospheric simulations using a GCM with simplified physical parameterizations. I. Model climatology and variability in multi-decadal experiments. *Climate Dyn.,* **20,** 175–191.

Münnich, M., and J. D. Neelin, 2005: Seasonal influence of ENSO on the Atlantic ITCZ and equatorial South America. *Geophys. Res. Lett.,* **32,** L21709, doi:10.1029/2005GL023900.

Murtugudde, R., J. P. McCreary, and A. J. Busalacchi, 2000: Oceanic processes associated with anomalous events in the Indian Ocean with relevance to 1997–1998. *J. Geophys. Res.,* **105,** 3295–3306.

Parthasarathy, B., A. A. Munot, and R. Kothawale, 1995: Monthly and seasonal rainfall series for all-India homogeneous regions and meteorological subdivisions: 1871–1994. Indian Institute of Tropical Meteorology Research Rep. 065, Pune, India, 10 pp.

Rao, A. S., S. K. Behera, Y. Masumoto, and T. Yamagata, 2002: Interannual variability in the subsurface tropical Indian Ocean. *Deep-Sea Res. II,* **49,** 1549–1572.

Rasmusson, E. M., and T. H. Carpenter, 1983: The relationship between the eastern Pacific sea surface temperature and rainfall over India and Sri Lanka. *Mon. Wea. Rev.,* **111,** 517–528.

Rayner, N. A., D. E. Parker, E. B. Horton, C. K. Folland, L. V. Alexander, D. P. Rowell, E. C. Kent, and A. Kaplan, 2003: Global analyses of sea surface temperature, sea ice, and night marine air temperature since the late nineteenth century. *J. Geophys. Res.,* **108,** 4407, doi:10.1029/2002JD002670.

Saji, N. H., and T. Yamagata, 2003: Structure of SST and surface wind variability during Indian Ocean dipole mode events: COADS observations. *J. Climate,* **16,** 2735–2751.

——, B. N. Goswami, P. N. Vinayachandran, and T. Yamagata, 1999: A dipole mode in the tropical Indian Ocean. *Nature,* **401,** 360–363.

Slingo, J. M., and H. Annamalai, 2000: 1997: The El Niño of the century and the response of the Indian summer monsoon. *Mon. Wea. Rev.,* **128,** 1778–1797.

Sperber, K. R., and T. N. Palmer, 1996: Interannual tropical rainfall variability in general circulation model simulations associated with the atmospheric model intercomparison project. *J. Climate,* **9,** 2727–2750.

Ting, M., and L. Yu, 1998: Steady response to tropical heating in wavy linear and nonlinear baroclinic models. *J. Atmos. Sci.,* **55,** 3565–3582.

Torrence, C., and P. J. Webster, 1999: Interdecadal changes in the ENSO–monsoon system. *J. Climate,* **12,** 2679–2690.

Walker, G. T., 1924: Correlations in seasonal variations of weather, IX. *Mem. India Meteor. Dept.,* **24,** 275–332.

Wang, B., I.-S. Kang, and J. Y. Lee, 2004: Ensemble simulations of Asian–Australian monsoon variability by 11 AGCMs. *J. Climate,* **17,** 4073–4090.

——, Q. Ding, X. Fu, I.-S. Kang, K. Jin, J. Shukla, and F. Doblas-Reyes, 2005: Fundamental challenge in simulation and prediction of summer monsoon rainfall. *Geophys. Res. Lett.,* **32,** L15711, doi:10.1029/2005GL022734.

Webster, P. J., and S. Yang, 1992: Monsoon and ENSO: Selectively interactive systems. *Quart. J. Roy. Meteor. Soc.,* **118,** 877–926.

——, A. M. Moore, J. P. Loschnigg, and R. R. Leben, 1999: Coupled ocean–atmosphere dynamics in the Indian Ocean during 1997–98. *Nature,* **401,** 356–360.

Wu, R., and B. P. Kirtman, 2004: Understanding the impacts of the Indian Ocean on ENSO variability in a coupled GCM. *J. Climate,* **17,** 4019–4031.

——, and ——, 2005: Roles of Indian and Pacific Ocean air–sea coupling in tropical atmospheric variability. *Climate Dyn.,* **25,** 155–170.

Zebiak, S. E., 1993: Air–sea interaction in the equatorial Atlantic region. *J. Climate,* **6,** 1567–1586.